Journal of the Korean Physical Society, Vol. 63, No. 1, July 2013, pp. 47∼52

Effects of Metallic Contaminant Type and Concentration on Photovoltaic Performance Degradation of p-type Silicon Solar Cells

In-Ji Lee
Department of Advanced Materials & Chemical Engineering, Hanyang University, Seoul 133-791, Korea

Ungyu Paik
Department of Energy Engineering, Hanyang University, Seoul 133-791, Korea

Jea-Gun Park*
Department of Electronic Engineering, Hanyang University, Seoul 133-791, Korea

(Received 26 February 2013, in final form 25 March 2013)

We investigated the effects of the metallic contaminant type and concentration (Al, Cu, Ni, and Fe) on the minority-carrier recombination lifetime and photovoltaic performance degradation of p-type silicon solar cells. For all contaminants, the lifetime after annealing at 900 °C for 15 min decreased with increasing concentration. The sequence of higher lifetime degradation induced by metallic contamination was Al (highest), Cu, Ni, and Fe (lowest), mainly determined by causing the diffusivity length and the solubility of the metallic contaminant in silicon. The sequence of higher lifetime degradation sensitivity induced by metallic contamination was Fe, Ni, Cu, and Al, as mainly determined by the trap energy level of the metallic contaminant in silicon. The contamination degraded the power-conversion efficiency (PCE) due to both the short-circuit-current and the fill-factor degradation. The degree and sensitivity of the PCE degradation depended on the contaminant type and concentration. The degree was the highest for Al, followed by Cu, Ni, and Fe, while the sensitivity was the highest for Fe, followed by Ni, Cu, and Al.

PACS numbers: 66.30.Jt, 73.20.Hb, 72.20.Jv, 61.72.Yx
Keywords: Silicon solar cell, Semiconductor, Diffusion, Defect, Trapping, Gettering
DOI: 10.3938/jkps.63.47

I. INTRODUCTION

The reduction in price of polysilicon has recently been a key engineering goal in the silicon solar industry because polysilicon accounts for the highest proportion of the production cost. This has led silicon solar-cell manufacturers to use solar-grade (SoG) or upgraded metallurgical grade (UMG) polysilicon, which contains many metallic impurities [1, 2]. These impurities greatly degrade photovoltaic performances such as the short-circuit current (J_{SC}), the open-circuit voltage (V_{OC}), the fill factor (FF) and the power conversion efficiency (PCE)in silicon solar cells [3–5]. Manufacturers are,thus, working to minimize or control metallic contamination of materials used in their fabrication processes, even when those processes use lower grade polysilicon. Recent studies have focused on the relationship between metallic contamination and the minority-carrier recombination lifetime or that between metallic contamination and photovoltaic performance. We have investigated the relationship between the metallic contaminant concentration and the minority-carrier recombination lifetime and that between the metallic contaminant concentration and photovoltaic performance for impurities with fast diffusivity (copper, nickel), middle diffusivity (iron), and slow diffusivity (aluminum).

II. EXPERIMENT

Boron-doped (10 Ω·cm) Czochralski (CZ) silicon wafers (50 × 50 mm^2)with a thickness of 200 μm were used. The detailed experimental flow is outlined in Fig. 1. The wafers were textured using KOH (potassium hydroxide) for 10 min, resulting in a random pyramid surface structure. After the texturing process, the wafers were subjected to $POCl_3$ diffusion at 860 °C for 5 min to produce an n^+ doping layer with a depth of ∼480 nm and an emitter sheet resistance of 58 Ω/□. The wafers were then cleaned in an SC2 (HCl-H_2O_2-H_2O mixture)

*E-mail: parkjgL@hanyang.ac.kr; Fax: +82-2-2296-1179

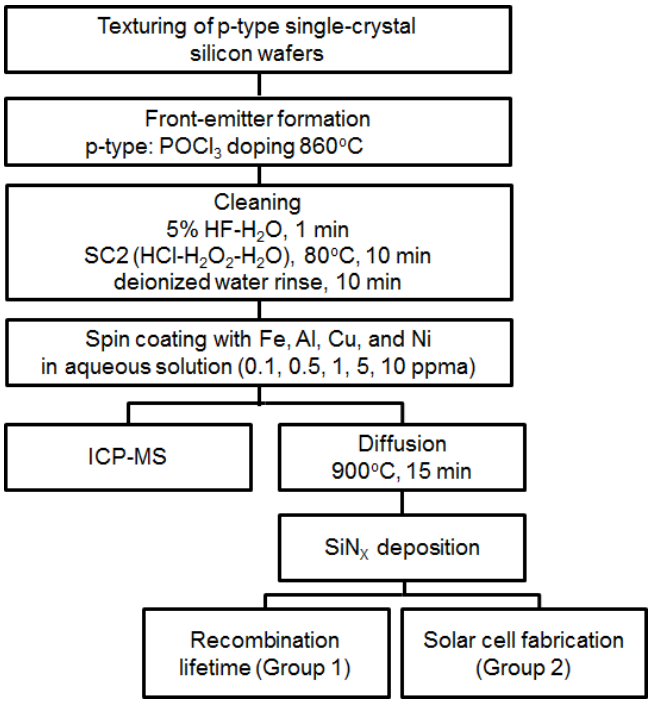

Fig. 1. Schematic process flow for the minority-carrier recombination lifetime measurement of p-type silicon wafers following by intentional metallic contamination,annealing and p-type silicon solar-cell fabrication.

solution to remove the initial contamination. Standard aqueous solutions of Al, Cu, Ni, and Fe (from Kanto Kagaku) at ∼1000 ppma were diluted with deionized water mixed with 2% HNO_3 to produce 0.1-, 0.5-, 1.0-, 5.0-, and 10.0-ppma aqueous solutions. An Al aqueous solution (1.6 ml) with a concentration of 0.1, 0.5, 1.0, 5.0, or 10.0 ppma was dropped on to the pyramid-textured silicon-wafer surface while a Ni, Cu,or Fe aqueous solution (1.6 ml) with a concentration of 0.1, 0.5, 1.0, 5.0, or 10.0 ppma was dropped on to its backside. The wafers were then spindriedat 600 rpm for 130 seconds. One complete set of contaminated wafers was subjected to an inductively-coupled-plasma mass spectrometry (ICP-MS) analysis to estimate the surface contamination concentration. Another complete set was heated at 900 °C for 15 min in order to drive the metallic contaminants on the surface into the silicon bulk. The Al diffused from the surface while the Cu, Ni, and Fe diffused from the backside.

A silicon-nitride film with a thickness of 80 nm was deposited under the same conditions by using low-frequency plasma-enhanced chemical vapor deposition (PECVD).The wafers with SiN_X films deposited wafers were separated into two groups. The minority-carrier recombination lifetimes of the wafers in the first group were estimated using quasi-steady-state photoconductance (QSSPC) and microwave-induced photoconductive decay (μ-PCD). QSSPC is an excellent method for measuring a wide range of minority-carrier lifetimes (from

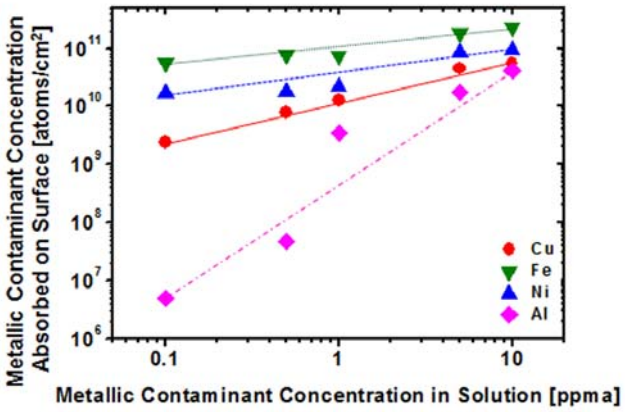

Fig. 2. (Color online) Dependence of the metallic contaminant concentration absorbed on wafer surface on the metallic contaminant concentration in solution after spin-coating solutions with Al, Cu, Ni, and Fe on the silicon wafer surface.

0.1 μs to several ms) over a wide range of carrier densities (10^{12}–10^{17} cm^{-3}), thereby revealing the minority-carrier recombination lifetime from the wafer surface to the backside. The micro-photoconductance decay (μ-PCD) caused by excess carriers generated by the absorbed light through the wafer surface from a flash lamp was measured by inductive coupling microwave heating using an RF coil under the sample. The μ-PCD detected the photoconductance via the reflection of microwavesat a wavelength of 904 nm, revealing the minority-carrier recombination lifetime from the wafer surface to a depth of ∼30 μm.

The wafers in the second group were subjected to screen-printing using Al and Ag pastes on the back and the front to produce top and bottom electrodes, respectively, for silicon solar cells. After having been screen-printed, the wafers were firedat 680 °C for 2 s by using rapid thermal annealing. Their photovoltaic performances(short-circuit current density (J_{SC}), open-circuit voltage (V_{OC}), fill factor (FF), and power-conversion efficiency (PCE)) were estimated using a solar simulator (Newport) under one sun global solar spectrum of air mass conditions(1.5).

III. EXPERIMENTAL RESULTS AND DISCUSSION

Figure 2 shows the metallic contaminant concentration absorbed on the wafer surface after spin coating as a function of the metallic contaminant concentration in the solution. For all four contaminants, the amount absorbed on the surface increased with increasing concentration in the solution. The degree of absorption was the highest for Fe, followed by Ni, Cu, and Al, at each concentration in the solution. These results are attributed to the reduction potential of a metallic contaminant in

an aqueous solution [6]. A negative reduction potential means a preferred oxidation while a positive one means a preferred reduction; the potentials were −0.04, −0.25, 0.340, and −1.662 V for Fe, Ni, Cu, and Al, respectively. A lower negative or positive reduction potential lead to a higher oxidation or reduction, which results in a higher metallic contaminant concentration absorbed on the wafer surface after spin coating. Thus, the highest surface absorption degree for Fe, followed by Ni, Cu, and Al,at each metallic contaminant concentration in the solution was due to the sequence of lower relative reduction potential being in the order Fe, Ni, Cu, and Al. Furthermore, the surface absorption sensitivity of metallic contaminants is given by

$$S(\text{surface absorbption sensitivity}) = \frac{dC_1}{dC_2}, \qquad (1)$$

where C_1 and C_2 are the metallic contaminant concentration absorbed on the surface and the metallic contaminant concentration in the solution, respectively. The sequence of surface absorption sensitivity from highest to lowest was Al (0.65), Cu (0.23), Ni (0.13), and Fe (0.10).

Figure 3 shows the dependence of the minority-carrier recombination lifetime on the metallic contaminant type and concentration as measured by using QSSPC and μ-PCD. A flashlight was used as the QSSPC light source. As mentioned above, QSSPC is an excellent method for measuring a wide range of minority-carrier lifetimes over a wide range of carrier densities for an entire wafer. A laser light source (λ = 904 nm)was used for the μ-PCD measurement, which measured the minority-carrier recombination lifetime in the wafer within 30 μm of the surface. The minority-carrier recombination lifetimes were degraded, compared to the reference (without surface metallic contamination), for all four contaminants and decreased with increasing metallic contaminant concentration.

The lifetime degradation sensitivity due to metallic contamination is given by

$$\frac{d\tau_n}{dC}, \qquad (2)$$

where τ_n and C are the minority-carrier recombination lifetime and the metallic contaminant concentration on the wafer surface. The Fe had the highest lifetime degradation sensitivity (3.122), followed by Ni (2.400), Cu (0.741), and Al (0.407). This is attributed to the trap energy level of the contaminant. Metallic impurities work as recombination centers in silicon bulk and create a trap energy level (E_t). The Shockley-Read-Hall recombination lifetime for a low concentration of injected impurities is given by [7,8]

$$\begin{aligned} \tau_{SRH} &= \frac{\tau_{n_0}(p_0 + p_1 + \Delta n) + \tau_{p_0}(n_0 + n_1 + \Delta n)}{p_0 + n_0 + \Delta n} \\ &\approx \frac{\tau_{n_0}(p_0 + p_1) + \tau_{p_0}(n_1 + \Delta n)}{p_0}, \end{aligned} \qquad (3)$$

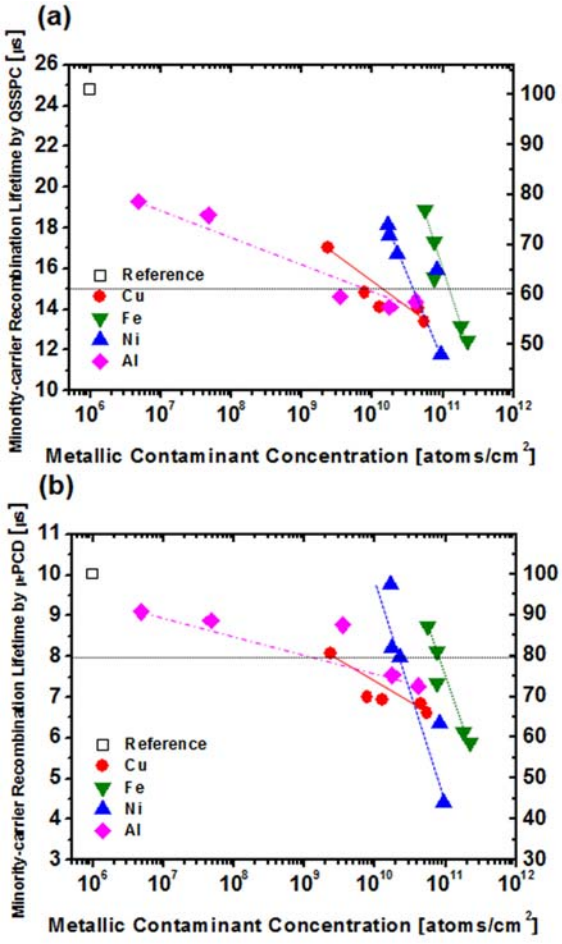

Fig. 3. (Color online) Dependencies of the degree of minority-carrier recombination lifetime degradation and the sensitivity on the metallic contaminant type and concentration as estimated by using (a) QSSPC and(b) μ-PCD.

where $\tau_{n_0} = (N_t \sigma_n v_{th,n})^{-1}$ and $\tau_{p_0} = (N_t \sigma_p v_{th,p})^{-1}$. The N_t, σ_n, σ_p, $v_{th,n}$, and $v_{th,p}$ are the trap concentration, capture cross-section for electrons, capture cross-section for holes, hole thermal velocity, and electron thermal velocity, respectively. In particular,τ_{SRH} is determined by the hole (p_1) and the electron (n_1) concentrations of the trap energy level:

$$p_1 = N_V \exp\left(-\frac{E_t - E_V}{kT}\right), \qquad (4)$$

$$n_1 = N_C \exp\left(-\frac{E_C - E_t}{kT}\right), \qquad (5)$$

where N_C, N_V, E_t, E_V, E_C, k, and T are the effective conduction band density of states, effective valence band density of states, energy of a trap, energy of the valence band edge, energy of the conduction band edge, Boltzmann's constant, and temperature, respectively. Thus, τ_{SRH} is determined by E_t; *i.e.*, a deep trap energy level (E_t) leads to a higher degradation of the carrier concentration at the trap energy level, resulting in a higher

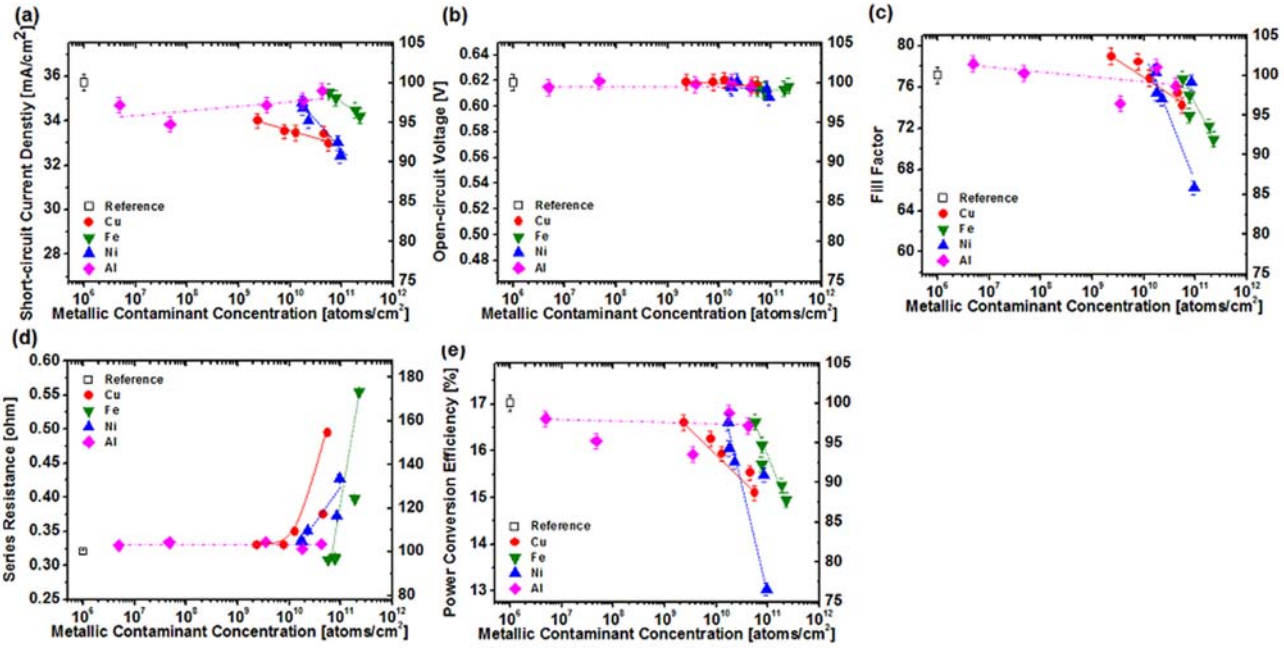

Fig. 4. (Color online) Dependence of the photovoltaic performance on the metallic contaminant type and concentration for p-type solar cells: (a) short-circuit current density (J_{SC}), (b) open-circuit voltage (V_{OC}), (c) fill factor (FF), (d) series resistance, and (e) power-conversion efficiency.

lifetime degradation sensitivity. The value of E_t for Fe, Ni, Cu, and Al are E_c-0.51 eV, E_C-0.35, E_C-0.2, and E_V + 0.069 eV, respectively [8–10]. Thus, the sequence of higher lifetime degradation sensitivity is Fe, Ni, Cu, and Al. Surprisingly, however, the sequence of higher lifetime degradation degree induced by metallic contaminant at a lifetime of 15 μs was Al, Cu, Ni, and Fe, which is the inverse of the sequence for higher lifetime degradation sensitivity, as shown in Fig. 3(a). This result is attributed to the diffusion length and solubility in silicon of metallic contaminants after annealing at 900 °C for 15 min. Note that the Cu, Ni,and Fe diffused from the wafer's backside while the Al diffused from the wafer's surface. The calculated diffusion lengths of Cu, Ni, Fe, and Al are 4.9×10^3, 1.3×10^3, 1.0×10^2, and 1.9×10^{-2} μm, respectively [8–10]. The Cu and the Ni were located near the wafer's surface after annealing because the diffusion lengths were larger than the wafer's thickness (180 μm). The Al was located near the wafer's surface after annealing because its diffusion was extremely low. In contrast, the Fe was located near the wafer's bulk center. At 900 °C, the solubilities of Cu, Ni, Fe, and Al were 2.2×10^{17}, 7.5×10^{16}, 4.3×10^{13}, and $\sim 9.1 \times 10^{18}$ atoms/cm^3, respectively [8–11]. The minority-carrier recombination lifetime is determined by the surface and bulk recombinations, as given by [7,8]

$$\frac{1}{\tau_{total}} = \frac{1}{\tau_{surface}} + \frac{1}{\tau_{bulk}}, \qquad (6)$$

where τ_{total}, $\tau_{surface}$, and τ_{bulk} are the total, surface, and bulk minority-carrier recombination lifetimes, respectively. The diffusion length and the solubility of the metallic contaminants determined the location and the recombination rate after annealing and indicated that Cu, Ni, and Al mainly affect the surface recombination lifetime while Fe affects the bulk lifetime. Since Cu and Ni prefer to form silicides at the surface (such as Cu_3Si and $NiSi_2$) [12–17] while Fe prefers to form $FeSi_2$ and FeB in the silicon bulk [16–22], the lifetime degradation degree induced by Al was the highest among the contaminants because Al was located nearest the wafer's surface and had the highest solubility in silicon. The next highest degrees were induced by Cu and Ni because Cu was located at the wafer's surface and was closer to it than Ni and because the solubility of Cu is higher than that of Ni. The lifetime degradation induced by Fe was the lowest because Fe was located near the wafer's bulk and has a lower solubility than Cu and Ni. The dependencies of the minority-carrier recombination lifetime degradation degree and sensitivity on the metallic contaminant type and concentration were also estimated by using μ-PCD.As shown in Fig. 3(b),the sequences of higher lifetime degradation sensitivity and degree estimated by using μ-PCD were the same as those estimated by using QSSPC.

Figure 4 shows the dependences of the photovoltaic performances on the metallic contamination type and concentration. All contaminants reduced J_{SC} compared to that of the reference (without metallic contamination), as shown in Fig. 4 (a). Except for Al, J_{SC} decreased with increasing contaminant concentration. The

sequence of higher J_{SC} degradation sensitivity ($\frac{dJ_{SC}}{dC}$) was Fe, Ni, and Cu; Al followed a trend similar to the lifetime degradation sensitivity shown in Figs. 3(a) and (b). The relationship between J_{SC} and the minority-carrier recombination lifetime is given by [7,8]

$$J_{SC} = qg_nL_n = qg_n\sqrt{D_n\tau_n}, \quad (7)$$

where J_{SC} is proportional to the square root of the minority-carrier recombination lifetime, and the J_{SC} degradation sensitivity ($\frac{dJ_{SC}}{dC}$) is smaller than the lifetime degradation sensitivity ($\frac{d\tau_n}{dC}$). Thus, the sequence for higher J_{SC} degradation sensitivity was the same as that for higher lifetime degradation sensitivity, except for Al (compare Fig. 3(a) with Fig. 4(a)). Nondependence of J_{SC} degradation on the Al concentration was found because of the dopant compensation rule, which is given by [7,8]

$$n = N_D - N_A = N_{phosphorus} - N_{aluminum}, \quad (8)$$

where n, N_D, N_A, $N_{phosphorus}$, and $N_{aluminum}$ are, respectively, the total electron concentration, donor concentration, acceptor concentration, phosphorous concentration, and Al concentration in the n^+ diffusion region of a silicon solar cell. According to this rule, the dependence of the J_{SC} degradation on the Al concentration cannot be undetermined because the phosphorous concentration of the n^+ diffusion region in a p-type silicon solar cell ($\sim 8\times10^{20}$ cm^{-3}) is much higher than the Al concentration after annealing at 900 °C for 15 min($\sim$9.1 $\times$ 10^{18} atoms/cm^3) and because the depth of the n^+ diffusion region ($\sim$0.58 μm) is deeper than the diffusion length of Al after annealing(only 1.9×10^{-2} μm).

For all metallic contaminants, the V_{OC} degradation was independent of the metallic contaminant concentration, as shown in Fig. 4(b). The FF decreased with increasing metallic contaminant concentration, as shown in Fig. 4(c). The sequence of higher FF degradation sensitivity ($\frac{dFF}{dC}$) was Fe, Ni, Cu, and Al, which is similar to the sequence of higher lifetime degradation sensitivity in Figs. 3(a) and (b). This result is attributed to the series resistance of p-type silicon solar cells, as shown in Fig. 4(d). The sequence of higher series resistance degradation sensitivity ($\frac{dR_S}{dC}$) was Fe, Ni, Cu, and Al, which is well correlated with the sequence of higher FF degradation sensitivity (Fig. 4(c)). The correlation between FF degradation sensitivity and series resistance is attributed to the Al being located in the n^+ diffusion region of a p-type silicon solar cell, Cu and Ni silicide being located near the front solar-cell surface, and Fe being located at the center of the silicon solar-cell bulk. However, the sequence of higher FF degradation degree was Al, Cu, Ni, and Fe, which is the reverse of the higher FF degradation degree sequence. Finally, the dependence of the PCE on the metallic contaminant type and concentration for p-type silicon solar cells is shown in Fig. 4(e). For all contaminants, PCE decreased with increasing metallic contaminant concentration. The sequence of higher PCE degradation degree was Al, Cu, Ni, and Fe. However, the sequence of higher PCE sensitivity ($\frac{dPCE}{dC}$) was Fe, Ni, Cu, and Al, which is well correlated with the sequence of higher lifetime, J_{SC}, and FF degradation sensitivity (Figs. 3(a), 4(a), and 4(c)). This indicates that metallic contaminants degrade not only J_{SC} but also FF and that the lifetime degradation induced by metallic contamination affects both J_{SC} and FF. In summary, the PCE degradation degree and sensitivity strongly depend on the metallic contaminant type and concentration.

IV. CONCLUSION

We have shown that metallic contaminants degrade the minority-carrier recombination lifetime in p-type silicon solar-cell wafers after annealing. The degree of lifetime degradation and the sensitivity induced by metallic contamination were determined by using the metallic contaminant type and concentration.The sequence of higher lifetime degradation sensitivity due to the trap energy level of the contaminants in silicon was Fe (highest), Ni, Cu, and Al (lowest).The sequence of the degree of higher lifetime degradation due to the location, as determined by using the diffusivity and the solubility of the contaminants after annealing, was the reverse (Al, Cu, Ni, and Fe).There was good correlation between the degree of lifetime degradation and the sensitivity and the degree of power-conversion efficiency (PCE) degradation and the sensitivity. The degree of PCE degradation and the sensitivity induced by metallic contamination were affected by both the short-circuit current density (J_{SC}) and the fill factor(FF) degradation. The J_{SC} degradation was attributed to the lifetime degradation induced by metallic contamination while the FF degradation was attributed to the series resistance in p-type solar cells. Therefore, the dependences of the degree of PCE degradation and the sensitivity on the metallic contaminant type and concentration in p-type silicon solar cells are mainly determined by the trap energy level, the solubility, and the diffusion length of metallic contaminants.

ACKNOWLEDGMENTS

This work was supported by the Brain Korea 21 Project in 2012 and by the Silicon Solar Consortium (SiSoC), an Industry/University Cooperative Research Center of the National Science Foundation.

REFERENCES

[1] A. Luque and S. Hegedus (Eds.), *Handbook of Photovoltaic Science and Engineering* (John Wiley & Sons, West Sussex,2003).

[2] C. P. Khattak, D. B. Joyce and F. Schmid, Production of solar-grade silicon by refining liquid metallurgical grade silicon, Annual Report NREL/SR-520-27593, December (1999), NREL.
[3] G. Coletti, P. C. P. Bronsveld, G. Hahn, W. Warta, D. Macdonald, B. Ceccaroli, K. Wambach, N. L. Quang and J. M. Fernandez, Adv. Funct. Mater. **21**, 879 (2011).
[4] J. R. Davis, A. Rohatgi, P. Rai-Choudhury, P. Blais, R. H. Hopkins and J. R. McCormick, *13thPhotovoltaic Specialists Conference* (Institute of Electrical and Electronics Engineers, Inc., New York, 1978).
[5] J. R. Davis, A. Rohatgi, P. Rai-Choudhury, P. Blais, R. H. Hopkins and J. R. McCormick, IEEE Trans. Electron Devices **27**, 677 (1980).
[6] K. A. Reinhardt and W. Kern (Eds.), *Handbook of Silicon Wafer Cleaning Technology* (William Andrew, Inc., New York, 2008).
[7] B. G. Streetman, *Solid State Electronic Devices* (Pearson Prentice Hall, New Jersey, 2006).
[8] S. M. Sze and Kwok K. Ng (Eds.), *Physics of Semiconductor Devices* (John Wiley & Sons, Inc., New Jersey, 2007).
[9] S. M. Sze (Ed.), *VLSI Technology* (McGraw-Hill, New York, 1988).
[10] K. Graff, *Metal Impurities in Silicon-device Fabrication* (Springer, Berlin-Heidelberg, 1995).
[11] T. Yoshikawa and K. Morita, J. Electrochem. Soc. **150**, G465 (2003).
[12] A. A. Istratov and E. R. Weber, Appl. Phys. A **66**, 123 (1998).
[13] A. A. Istratov and E. R. Weber, J. Electrochem. Soc. **149**, 21 (2002).
[14] J. G. Park, G. S. Lee, J. S. Lee, K. Kurita and H. Furuya, Mater. Sci. Eng. B **134**, 249 (2006).
[15] S. A. McHugo, A. Mohammed, A. C. Thompson, B. Lai and Z. Cai, J. Appl. Phys. **91**, 6396(2002).
[16] D. Macdonald, Appl. Phys. A **81**, 1619(2005).
[17] D. Macdonald L. J. Geerligs and A. Azzizi, Appl. Phys. Lett. **95**, 1021 (2004).
[18] J. G. Park, K. Kurita, G. S. Lee, S. A. Shin and H. Furuya, Microelectron. Eng. **66**, 247 (2003).
[19] A. A. Istratov, H. Hieslmair and E. R. Weber, Appl. Phys. A **70**, 489 (2000).
[20] D. Macdonald and L. J. Geerligs, Appl. Phys. Lett. **85**, 4061 (2004).
[21] M. Hourai, K. Murakami, T. Shigematsu, N. Fujino and T. Shiraiwa, Jpn. J. Appl. Phys. **28**, 2413 (1989).
[22] T. S. Horanyi, T. Pavelka and P. Tutto, Appl. Surf. Sci. **63**, 306 (1993).